99/104
Large-Deflection Coupled Torsion/Bending

1 Introduction

Recent work of Reismann[1] considers numerical analysis of the large-deflection due to coupled torsion/bending of a weightless cantilever. This published work provides an interesting case against which OrcaFlex can be validated.

The beam cross section is a narrow rectangle, $h/t = 10$, with a concentrated point load (P) applied at the cantilever tip. The key point is that the load is not exactly in the plane of the beam, but is offset at an angle γ (see the initial configuration illustrated in Figure 1). The notation here is that used in the OrcaFlex model.

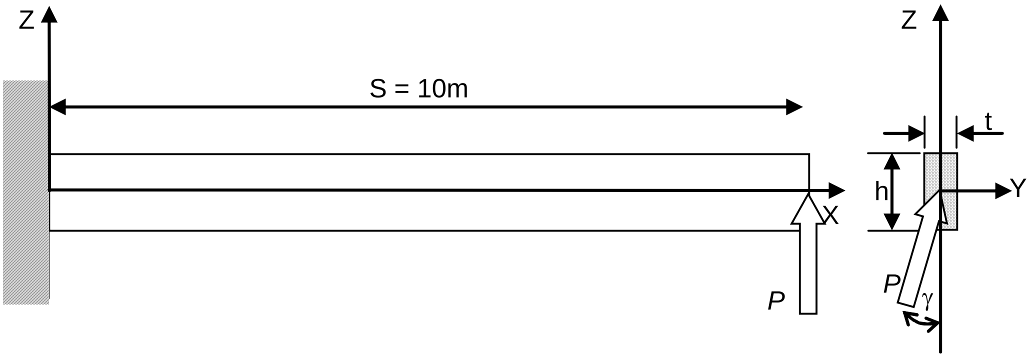

Figure 1: Initial Configuration

As the magnitude of the applied load P is increased, the cantilever starts to bend out-of-plane (see Figure 2), eventually reaching a buckling load where the lateral deflection increases rapidly. This elastic buckle is not catastrophic, and Reismann has found solutions extending well into the post-buckling region.

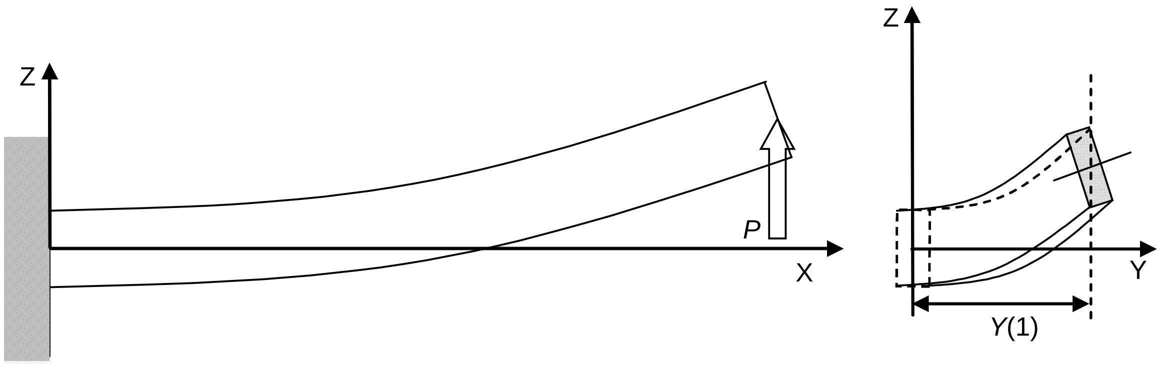

Figure 2: Deflected Shape

[1] *Three-dimensional finite inextensional deformation of a beam*, Herbert Reismann, International Journal Non-Linear Mechanics **35** (2000), 157-165.

Figure 2 clearly shows the effect on the deflected shape of the application of a non-centred load. Note how the cross section at the tip of the cantilever has not only been displaced vertically, but how a counter clockwise rotation has been introduced.

In Reismann's paper he presents two sets of results against which we will compare OrcaFlex results:

a) Reismann's Table 3: This is for the case of P = 4.0000, α=90°, β=89° and γ=1°, and gives a series of results as functions of arc length along the cantilever. In this article we will specifically compare OrcaFlex results for displacement co-ordinates and bending moment components.

b) Reismann's Figure 4: For a range of P ($0 \le P \le 5.4$) and γ (= 0°, 1/3°, 1°, 3°, and 5°), Reismann presents curves of lateral end deflection $Y(1)$. In this article we will compare results for the same range of P and with γ = 1°, 3°, and 5°.

2 OrcaFlex Model

When modelling this in OrcaFlex there are two main areas which require particular treatment:

1. The Reismann analysis is for the case of zero gravity. The latest versions of OrcaFlex do allow user-specification of the gravitational constant. However, this comparison work was performed with a prior version of OrcaFlex which did not include this capability.

   The solution chosen was to immerse the cantilever in water with a density 1000kg/m^3. We then give the cantilever a finite mass of 10kg/m and a cross-section diameter of 0.128379m. These combine to give precise neutral buoyancy. Note that there is no inconsistency between defining these data to give neutral buoyancy and defining the required non-isotropic properties of the beam, since the bending stiffnesses are entered as user-defined data items.

2. In order to apply the force to the cantilever tip, we attach an OrcaFlex 6-D Buoy of negligible mass and buoyancy. We can then specify the components of load in global axes.

3 Results

Reismann's results are presented in non-dimensional form, so we therefore have some freedom in the choice of an appropriate set of properties, eg:

- Beam span = 10 m
- EI_{xx} = 1.75 kNm^2
- EI_{yy}= 175 kNm^2
- GJ = 2.52 kNm^2

Reismann's non-dimensional constants are then:

$A = EI_{xx} = 0.8333\ Et^4$

$B = EI_{yy} = 83.333\ Et^4$

$$C = GJ = \frac{EJ}{2(1+\neg)} = 1.2\,Et^4 \text{ (taking Poisson's ratio } \nu = 0.3)$$

$$D = \frac{B}{\sqrt{AC}} = 83.333$$

$$F = \sqrt{A/C} = 0.8333.$$

3.1 Reismann Figure 4

Reismann presents a curve of *Y*(1) vs. Applied Load *P* in Figure 4 of his paper. There are five curves shown corresponding to γ = 0, 0.333, 1, 3, and 5 degrees. We have used the automation facilities of OrcaFlex to run 20 increments of static load for γ = 1°, 3° and 5°.

The OrcaFlex dimensional values are converted to Reismann's non-dimensional form using Reismann's non-dimensional constants from Table 2 of his paper.

Figure 3 compares the corresponding Reismann and OrcaFlex results: it can be seen that the agreement is excellent throughout the range.

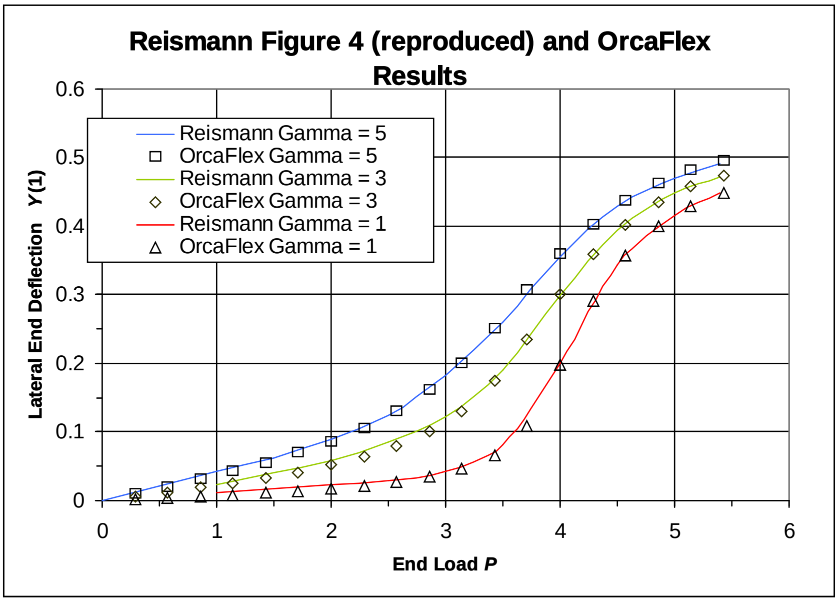

Figure 3

3.2 Reismann Table 3

For the particular case of *P* = 4.0000, α=90°, β=89° and γ=1°, Reismann has presented a series of results as functions of arc length measured along the cantilever. For this case OrcaFlex has been used to calculate the displacements and moments acting. The comparisons are shown in the figures below:

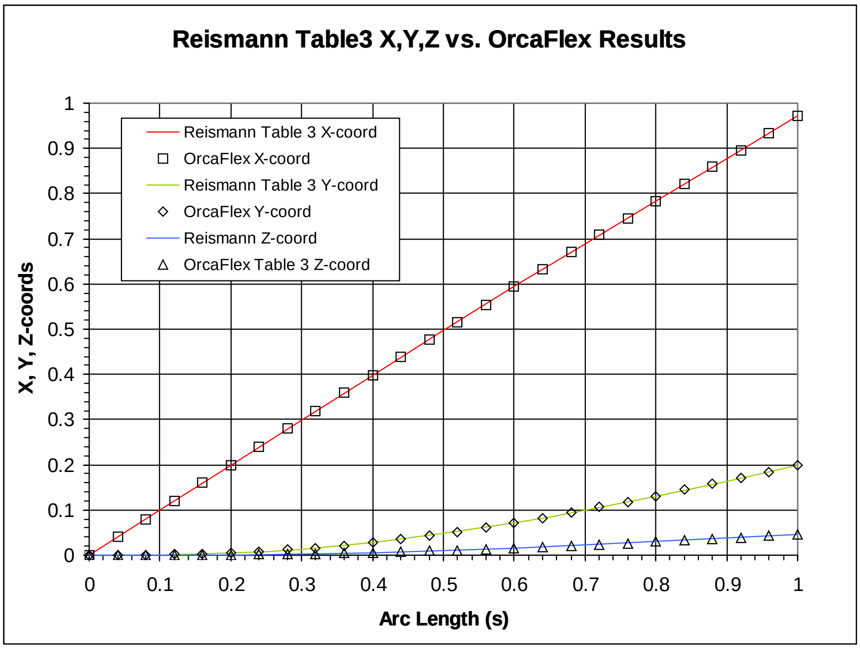

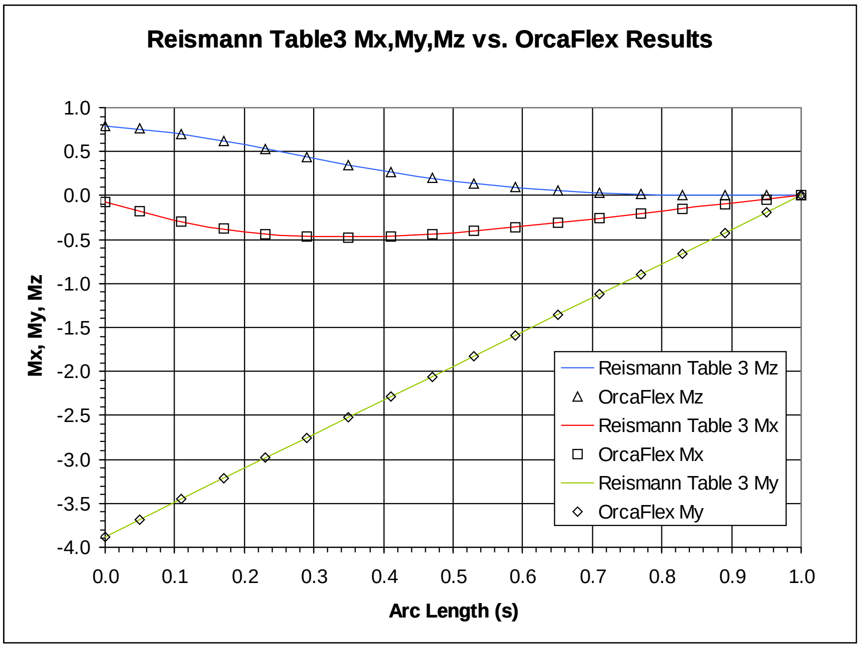

Figure 4: Reismann and OrcaFlex results for Reismann Table 3

4 Discussion

The deflection curves (figure 3) illustrate that for γ = 1° the cantilever shows an elastic instability starting at about P = 3.5 (= 74N load). Other results show that as γ is increased, the buckle is less abrupt: conversely it gets sharper as γ tends towards zero.

It is interesting to compare this with the classic instability case where the load is in plane, ie γ_p = 0. See, for example, Timoshenko and Gere: Theory of Elastic Stability, pg 260, eqn 6-23:

$$P_{crit} = 4.013\frac{\sqrt{EI_x C}}{L^2}$$

Note in this formula *C* = *GJ*. Then in our case, P_{crit} = 0.0843kN = 84.3N.

Incidentally, in the past we have used this case as a validation test for OrcaFlex. We have found that we can predict the critical load within 0.1% or 0.2%. However it is a tricky test to perform, because one is obliged to run repeated cases, increasing the load in very small increments, and testing for stability, dynamically, by applying a very small lateral disturbance.

It should also be noted that in order to perform the comparison with Reismann's work, as illustrated above, you must have the ability to set user defined non-isotropic bend stiffness for the line.

5 Acknowledgement

Our thanks go to Eugene Sas of Technip who drew our attention to Professor Reismann's work.